Proteinase-Activated Receptor 4 (PAR4) Activation Triggers Cell Membrane Blebbing through RhoA and β-arrestin.

Christina MG Vanderboor, Pierre E Thibeault, Kevin CJ Nixon, Robert Gros, Jamie Kramer and Rithwik Ramachandran.
Department of Physiology and Pharmacology, Schulich School of Medicine and Dentistry, University of Western Ontario, London, Ontario, Canada.

Correspondence and request for materials should be directed to:

Rithwik Ramachandran,
Department of Physiology and Pharmacology,
Schulich School of Medicine and Dentistry,
University of Western Ontario, London,
Ontario, Canada.
519-661-2142
rramach@uwo.ca

Abstract

Proteinase-Activated Receptors (PARs) are a four-member family of G-protein coupled receptors that are activated via proteolysis. PAR4 is a member of this family that is cleaved and activated by serine proteinases such as thrombin, trypsin and cathepsin-G. PAR4 is expressed in a variety of tissues and cell types including platelets, vascular smooth muscle cells and neuronal cells. In studying PAR4 signalling and trafficking, we observed dynamic changes in the cell membrane with spherical membrane protrusions that resemble plasma membrane blebbing. Since non-apoptotic membrane blebbing is now recognized as an important regulator of cell migration, cancer cell invasion, and vesicular content release we sought to elucidate the signalling pathway downstream of PAR4 activation that leads to such events. Using a combination of pharmacological inhibition and CRISPR/Cas9-mediated gene-editing approaches we establish that PAR4-dependent membrane blebbing occurs independently of the $G\alpha_{q/11}$ and $G\alpha_i$ signalling pathways and is dependent on signalling via the β-arrestin-1/-2 and RhoA signalling pathways. In order to gain a more comprehensive understanding of β-arrestin-mediated signalling downstream of PAR4 and to guide future studies, we undertook RNA-seq analysis of PAR4 activated genes in control cells and in cells lacking β-arrestin-1/-2. A list of differentially expressed genes was generated followed by Gene Ontology (GO) and enrichment analysis, revealing PAR4 regulation of genes involved in processes including blood coagulation and circulation, cell-cell adhesion, sensory perception and neuron-neuron synaptic transmission- terms that relate back to known functions of PAR4 and are consistent with our finding of membrane blebbing triggered by PAR4 activation. Together these studies provide further mechanistic insight into PAR4 regulation of cellular function.

Significance Statement

We find that the thrombin receptor PAR4 triggers cell membrane blebbing in a RhoA- and β-arrestin-dependent manner. In addition to identifying novel cellular responses mediated by PAR4, these data provide further evidence for biased signaling in PAR4 since membrane blebbing was dependent on some, but not all, signaling pathways activated by PAR4. Finally through CRISPR/Cas9-mediated targeting and RNA-seq analysis we catalogue here PAR4-dependent transcription that is dependent on β-arrestin.

Introduction

Proteinase activated receptors (PARs) are a four-member family of G-protein coupled receptors (GPCRs). PARs are unique among GPCRs, in being activated via proteolytic unmasking of a receptor-activating 'tethered ligand', that interacts intramolecularly with the orthosteric ligand binding pocket to trigger signalling (Ramachandran *et al.*, 2012) . PAR4, the most recently identified member of this family (Xu *et al.*, 1998), is expressed in a variety of tissues and cell types including the platelets, vascular smooth muscle cells, neuronal cells, and some cancer cells.

Much work has been done to develop PAR1- and PAR4-targeted compounds as anti-platelet agents. Both PAR1 and PAR4 are expressed in human platelets and both of these receptors are activated by the coagulation cascade enzyme thrombin. Importantly though, PAR1 and PAR4 appear to serve different roles in the platelet activation process (Kahn *et al.*, 1999), with PAR1 the high-affinity thrombin receptor playing an initiating role and the lower-affinity thrombin receptor PAR4 serving to consolidate and propagate the clot (Kahn *et al.*, 1999). The PAR1 antagonist voropaxar (zontivity), while highly effective in reducing cardiovascular complications, exhibited significant side effects with an elevated risk for bleeding including in the brain (Morrow *et al.*, 2012), further spurring recent efforts to target PAR4. Recent work with small molecule PAR4 antagonists has supported the idea that PAR4 antagonists are effective in reducing platelet rich thrombus formation in human platelets *ex vivo* (Wilson *et al.*, 2017) and in rodent and non-human primate models *in vivo* (Wong *et al.*, 2017). In non-human primate models, PAR4 blockade was associated with low bleeding liability and had a markedly wider therapeutic window compared to the commonly used antiplatelet agent clopidogrel (Wong *et al.*, 2017).

In keeping with emerging literature for other GPCRs, we now know that activated PAR4 can directly couple to multiple G-protein-signalling pathways including $G\alpha_{q/11}$ and the $G\alpha_{12/13}$ pathway (Woulfe, 2005; Kim *et al.*, 2006) but is thought not to engage $G\alpha_i$ dependent signalling pathways (Kim *et al.*, 2006). PAR4 can also recruit and signal through β-arrestins (Li *et al.*, 2011; Ramachandran *et al.*, 2017). In recent work, we identified a C-terminal motif in PAR4 that was critical for PAR4 signalling through the $G\alpha_{q/11}$ calcium signalling pathway and for recruiting β-arrestin-1/-2 (Ramachandran *et al.*, 2017). The mutant receptor with an 8-amino acid C-terminal deletion (dRS-PAR4) failed to internalize following activation with the PAR4 agonists thrombin or AYPGKF-NH_2 suggesting a role for β-arrestins in PAR4 trafficking. A pepducin targeting this C-terminal motif was also effective in attenuating PAR4-dependent platelet aggregation and thrombosis *in vivo* (Ramachandran *et al.*, 2017). These recent findings point to the exciting possibility that it might be possible to therapeutically target PAR4 signalling in a pathway-specific manner. The present study was spurred by our observations that PAR4 activation rapidly triggered the formation of dynamic membrane blebs, which were absent in dRS-PAR4 expressing cells.

Non-apoptotic plasma membrane blebbing is now recognized as a feature of various cellular processes including directional cellular migration during development, cancer cell migration and invasion, neuronal cell remodeling, and vesicular content release (Charras, 2008; Charras and Paluch, 2008; Charras *et al.*, 2008). Blebs are formed when the plasma

membrane transiently detaches from the underlying actin filaments resulting in intracellular pressure-mediated spherical membrane protrusions (Charras *et al.*, 2008; Tinevez *et al.*, 2009). The reassembly of actin filaments limits the expansion of blebs and actin polymerization while actomyosin contraction drives the retraction of the blebs (Charras *et al.*, 2008). The molecular signals that trigger the formation of membrane blebs are begining to be understood and include signalling from cell surface receptor such as GPCRs and receptor tyrosine kinases (Hagmann *et al.*, 1999; Lawrenson *et al.*, 2002; Godin and Ferguson, 2010; Chen *et al.*, 2012; Laser-Azogui *et al.*, 2014). A role for multiple Rho isoforms has also been described in regulating various aspects of bleb formation and retraction (Pinner and Sahai, 2008; Aoki *et al.*, 2016; Gong *et al.*, 2018). Previous work has described regulation of Rho-signalling by GPCRs in both a G-protein- and β-arrestin-dependent manner (Sah *et al.*, 2000; Barnes *et al.*, 2005; Anthony *et al.*, 2011).

Here we examine in detail the pathways leading from PAR4 to the formation of membrane blebs. We find that inhibition of $G\alpha_{q/11}$ signalling had no effect on the formation of PAR4 triggered membrane blebs, while blockade of β-arrestin-1/-2- or Rho-dependent signalling significantly reduced blebbing.

Materials and Methods

Materials

DMEM, trypsin-EDTA (0.25%), PBS, Penicillin-Streptomycin and sodium pyruvate were purchased from Thermo Fisher (Waltham, MA). Peptide ligands were custom synthesized by Genscript (Piscataway, NJ) at greater than 95% purity. Thrombin was purchased from Calbiochem (Oakville, ON), coelanterazine-h was from Nanolight Technology (Pinetop, AZ). All antibodies (anti-β-arrestin-1/-2, anti-RhoA, anti-actin, anti-rabbit-HRP) used in this study were purchased from Cell Signalling Technologies. YM254890 was from Wako chemicals (Richmond, VA), GSK269962 was from Tocris (Oakville, ON) and all other chemicals were from Sigma-Aldrich (Oakville, ON).

Cell Culture and transfections

HEK-293 (ATTC) cells were maintained in DMEM (Gibco) with 10% fetal bovine serum (Gibco), 1% penicillin-streptomycin (Gibco) and 1% sodium pyruvate (Gibco). Cells stably expressing PAR4-YFP or PAR4-dRS-YFP were maintained in the above media supplemented with 600 μg/mL of geneticin (Gibco). Cells were transiently transfected using a modified calcium phosphate method (Ferguson and Caron, 2004). Experiments were performed 48 hours post transfection. Primary rat smooth muscle cells were isolated and cultured as previously described (Gros *et al.*, 2006).

Creation of β-arrestin-1/-2 and RhoA knockout cells.

RhoA and β-Arrestin-1/-2 knock out HEK-293 cells (RhoA-KO HEK and β-arrestin-1/-2-KO HEK respectively) were generated using CRISPR/Cas9 mediated gene targeting. Guides targeting the β-arrestins or RhoA were designed using the design tool at http://crispr.mit.edu. Gene specific guides (β-arrestin 1; TGTGGACCACATCGACCTCG, β-arrestin 2; GCGGGACTTCGTAGATCACC and RhoA; CGAGTTTGCGACTCGCGGAC, CGGTCCGCGAGTCGCAAACT,

147 GAGTCCAGCCTCTTCGCGCC, GACTCGCGGACCGGCGTCCC) were ligated into the
148 PX458 vector (a kind gift from Dr. Feng Zhang, MIT, Addgene plasmid # 48138), verified
149 by direct sequencing and transfected in HEK cells via the calcium phosphate method. 48
150 hours post transfection, GFP expressing single cells were flow sorted into individual wells
151 of a 96 well (Becton Dickinson FACSAria III). Clonal cells from individual wells were
152 screened by western blotting to identify cell lines which were deficient in β-arrestin 1/2 or
153 RhoA (Supplementary Figure 1).
154
155 **Confocal microscopy**
156 Cells were plated onto glass bottom 35 mm dishes (MatTek, Ashland, MA) and imaged
157 using Zeiss LSM 510 Meta NLO confocal microscope. Yellow fluorescent protein was
158 excited with 514 laser line and visualized with 535-560 filter set. mCherry fluorophore was
159 excited with 543 laser line and visualized with 560-590. Green fluorescent protein was
160 excited with 488 laser line and visualized with 530-560 filter set. Cell shape change
161 experiments were conducted as follows. Cells were treated with vehicle or inhibitor as
162 indicated in the figure legends and incubated at 37°C. Plates were then placed on a heated
163 stage on the microscope and PAR4 was activated with AYPGKF-NH_2 (30μM) or thrombin
164 (3U/ml). 6-12 images per dish were taken over 10 minutes. Images were analyzed by
165 manually counting cells displaying membrane protrusions or blebs versus cells that did not
166 display any membrane protrusions.
167
168 **Bioluminescent Resonance Energy Transfer (BRET) assay for β-arrestin-1/-2**
169 **recruitment.**
170 Bioluminescent resonance energy transfer was measured between c-terminally YFP tagged
171 PAR4 (Ramachandran *et al.*, 2017) and Renilla Luciferase (Rluc) tagged β-arrestin-1 or β-
172 arrestin-2 (a kind gift from Dr. Michel Bouvier, U. de Montreal), following 20 minutes of
173 receptor activation as described in previous studies (Ramachandran *et al.*, 2009). Briefly,
174 PAR4-YFP (1 μg) and β-arr-1-Rluc and -2-Rluc) (0.1μg) were transiently transfected in
175 cells plated in a six well plate for 24 hours. Cells were re-plated into white 96-well culture
176 plates and cultured for a further 24 hours. Interactions between PAR4 and β-arrestin-1/-2
177 were detected by measuring the BRET ratio at timed intervals over 20 min following the
178 addition of 5 μM coelenterazine (Nanolight Technology, Pinetop, AZ) on a Mithras
179 fluorescence plate reader (Berthold) in luminescence mode using the appropriate filters.
180
181 **RNA-seq PAR4 transcriptome analysis in control and β-arrestin-1/-2 knockout HEK-**
182 **293 cells.**
183 HEK-293 cells or β-arrestin-1/-2-KO HEK cells stably expressing PAR4-YFP were treated
184 with 30μM AYPGKF-NH_2 for 2 hours. RNA was extracted using an RNeasy mini kit
185 (Qiagen) and analyzed on a bioanalyzer (Agilent, Santa Clara, CA). Sequencing libraries
186 were generated using the ScriptSeq complete kit which incorporated the Ribo-Zero
187 ribosomal RNA (rRNA) removal technology. Sequencing was done on a NextSeq
188 (Illumina) at the London Regional Genomics Centre.
189
190 **Sequencing Analysis**
191 Raw sequencing reads were trimmed using Prinseq quality trimming (Schmieder and
192 Edwards, 2011) with a minimum base quality score of 30. Read quality was then assessed

using FastQC (http://www.bioinformatics.babraham.ac.uk/projects/fastqc). Trimmed reads were then aligned to the *Homo sapiens* reference genome (CRCh release 38) using the STAR RNA-Seq aligner (Dobin *et al.*, 2013). An average of 28,049,697 and 20,706,493 high quality uniquely aligned reads with a maximum of four mismatches were obtained from HEK-293 cells and β-arrestin-1/-2-KO-HEK cells respectively. (Table 1 and Figure S2 and S3). The number of reads per gene was quantified by inputting reads that uniquely aligned to the reference genome with a maximum of four mismatches into HTSeq-count (Anders *et al.*, 2015) with the - type flag indicating 'gene' (Table 1 and Figure S2 and S3). Genes associated with rRNA and non-protein coding genes were removed from the analysis and genes with no reads across all samples in the count tables were removed from analysis leaving 18,615 genes for downstream analysis. Raw gene counts were normalized and differential expression analysis between HEK-293 cells and β-arrestin-1/-2-KO HEK cells with and without the treatment of 30μM AYPGKF-NH_2 was performed using the R (R: A language and environment for statistical computing. Vienna, Austria: R Foundation for Statistical Computing; 2017) package DESEQ2 (Love *et al.*, 2014). Differentially expressed genes were defined as genes with a fold-change >2 and a Benjamini-Hochberg adjusted p-value <0.05. Overlap between datasets was determined and visualized as a Venn diagram using BioVenn (Zhang *et al.*, 2009). Gene ontology (GO) enrichment analysis was performed on upregulated and downregulated differentially expressed genes with the Panther software (Mi *et al.*, 2017) on http://geneontology.org using the GO-SLIM function.

Accession numbers

The raw data for RNA-seq is available at the NCBI Gene Expression omnibus (GEO), accession number GSE134713.

Statistical Analysis. Statistical analysis of data and curve fitting were done with Prism 7 software (GraphPad Software, San Diego, CA). Statistical significance was assessed using the Student's t-test or Anova with Tukey's post-test.

Results

Activation of PAR4 elicits cell shape changes that are dependent on a C-tail eight-amino acid sequence.

Stimulation of plasma membrane localized PAR4-YFP in HEK-293 cells stably expressing PAR4-YFP with the PAR4 specific peptide agonist AYPGKF-NH_2 resulted in cell shape changes (Fig. 1A, B). PAR4 expressing cells treated with 30 μM AYPGKF-NH_2, displayed protrusions forming at the plasma membrane, indicated by arrows (Fig. 1B). These structures resemble membrane blebs and began to form around 2 minutes post agonist stimulation and lasted for up to 30 minutes in the presence of 30 μM AYPGKF-NH_2. In order to further verify that the cytoskeletal changes were indeed membrane blebs, we examined the effect of treating cells with Blebbistatin, a small molecule inhibitor of myosin II ATPase (Cheung *et al.*, 2002; Straight *et al.*, 2003) which functions by locking actin heads in a low actin affinity complex (Kovács *et al.*, 2004) and is reported to inhibit non-apoptotic membrane blebbing. Incubation of cells with blebbistatin significantly reduced the AYPGKF-NH_2-stimulated membrane bleb response in PAR4-YFP expressing HEK-293 cells (15.37% +/- 4.14) (Fig. 1C-E). In contrast, PAR4-YFP expressing cells treated with DMSO vehicle control displayed membrane blebs with a mean of 82.25% +/-

239 8.25. In recent studies we described a mutant PAR4 receptor lacking eight amino acids
240 from the C-tail, dRS-PAR4-YFP (Ramachandran *et al.*, 2017). We observed that in contrast
241 to the wild type receptor, dRS-PAR4-YFP expressing cells display significantly less
242 blebbing in response to 30 μM AYPGKF-NH_2 treatment (Fig. 2A-C). 82.33% +/- 1.2 of
243 HEK-293 cells stably expressing wild type PAR4-YFP displayed membrane blebbing as
244 opposed to 8.2% +/- 2.35 dRS-PAR4-YFP expressing cells, indicating that PAR4 triggered
245 membrane blebbing required the activation of signalling pathways that are dependent on
246 the eight-amino acid sequence in the C-tail of PAR4. Previously, we established that dRS-
247 PAR4-YFP does not couple to $G\alpha_{q/11}$ and is unable to recruit β-arrestins in response to
248 thrombin or AYPGKF-NH_2 activation (Ramachandran *et al.*, 2017). Since this mutant
249 receptor is also unable to activate blebbing, we hypothesized that PAR4 cell shape changes
250 are $G\alpha_{q/11}$- and/or β-arrestin-dependent and examined the effect of blocking these pathways
251 on bleb formation.
252
253 **PAR4-mediated cell shape change is $G\alpha_{q/11}$ and $G\alpha_i$ independent**
254 In order to determine whether PAR4 triggered blebbing is $G\alpha_{q/11}$-dependent, we
255 treated cells with the potent and selective $G\alpha_{q/11}$ inhibitor YM-254890 (Taniguchi *et al.*,
256 2004). It is well established that GPCRs couple to $G\alpha_{q/11}$ to mobilize calcium and activate
257 protein kinase C (PKC) (Exton, 1996; Wettschureck and Offermanns, 2005). Activated-
258 PKC translocation from the cytosol to the plasma membrane can be observed to monitor
259 this process (Dale *et al.*, 2001; Policha *et al.*, 2006). We employed this assay to visualize
260 the efficacy of YM-254890 in inhibiting $G\alpha_{q/11}$ signalling through PAR4. Cells were
261 transiently transfected with PAR4-mCherry and PKCβ1-GFP. PAR4 expression was
262 observed at the cell membrane and PKCβ1 expression was evident in the cytoplasm in
263 resting cells. Upon treatment with 30 μM AYPGKF-NH_2, PKCβ1-GFP translocated to the
264 membrane (Fig. 3A-C) and blebbing responses were observed, as before. In cells treated
265 with 100 nM YM-254890, PKCβ1-GFP failed to translocate to the membrane following
266 treatment with AYPGKF-NH_2. 100nM YM-254890 treated cells however maintained their
267 ability to bleb in response to AYPGKF-NH_2 (Fig. 3D-F). The role of $G\alpha_{q/11}$ in PAR4-
268 mediated blebbing was further quantified in HEK-293 cells stably expressing PAR4-YFP
269 treated with either DMSO vehicle or YM-254890 prior to stimulation with 30 μM
270 AYPGKF-NH_2. Blebbing in vehicle treated cells was not significantly different from cells
271 treated with YM-254890, 81.0% +/- 4.5 and 77.0% +/- 2.5 respectively (Fig. 3G). This
272 data indicates that YM-254890 functionally blocks $G\alpha_{q/11}$ signalling as indicated by a lack
273 of PKCβ1 translocation but does not block cell shape changes mediated by PAR4
274 activation.
275
276 HEK-293 cells, transiently expressing PAR4-mCherry with PKCβ1-GFP, showed
277 that activation of PAR4-mCherry with AYPGKF-NH_2 causes a translocation of PKCβ1-
278 GFP from the cytosol to the plasma membrane (Fig. 4A, B). In contrast, HEK-293 cells
279 transiently expressing dRS-PAR4-mCherry with PKCβ1-GFP showed that activation of
280 dRS-PAR4-mCherry does not cause a redistribution of PKCβ1-GFP to the membrane (Fig.
281 4C, D). Although PKC activation is downstream of $G\alpha_{q/11}$, since dRS-PAR4 does not
282 activate PKC and does not elicit cell shape changes, we tested PKC for a potential role in
283 mediating PAR4-mediated cell shape changes. HEK-293 cells stably expressing PAR4-

284 YFP were treated with the PKC inhibitor Gö6983 (Gschwendt *et al.*, 1996), prior to
285 stimulation with 30 μM AYPGKF-NH_2 and visualization by confocal microscopy. There
286 was no significant difference in the number of DMSO vehicle treated cells displaying
287 blebbing when compared to cells treated with Gö6983 in response to AYPGKF-NH_2,
288 74.5% +/- 4.6 and 72.2% +/- 9.2 (Fig. 4G). This data then suggests that neither $G\alpha_{q/11}$ or
289 PKC facilitate PAR4-mediated cell shape changes.
290
291 After ruling out $G\alpha_{q/11}$ as a potential signalling partner for PAR4-mediated
292 membrane blebs, we tested $G\alpha_i$ recruitment as a potential regulator of these responses
293 through inhibition of $G\alpha_i$ signalling with pertussis toxin. HEK-293 cells stably expressing
294 PAR4-YFP were incubated with pertussis toxin (100 nM) for 18 hrs prior to stimulating the
295 cells with 30 μM AYPGKF-NH_2. We did not observe any reduction in the number of cells
296 that displayed blebbing when compared to cells incubated with vehicle control (saline),
297 76.3% +/- 4.7 and 78.0% +/- 3.4 respectively (Fig. 5A-C).
298
299 **PAR4-mediated cell shape change is RhoA and ROCK dependent.**
300 Since RhoA can be activated by a $G\alpha_{q/11}$ and β-arrestin-1-dependent mechanism
301 following activation of the angiotensin II type 1 receptor (Barnes *et al.*, 2005) and since
302 RhoA is also well-established as a regulator of actin cytoskeleton rearrangements (Barnes
303 *et al.*, 2005; Aoki *et al.*, 2016), we examined whether PAR4-mediated blebbing was RhoA-
304 and ROCK-dependent. Treatment of PAR4-YFP expressing HEK-293 cells with the ROCK
305 specific inhibitor GSK269962 (Stavenger *et al.*, 2007) significantly reduced the number of
306 blebbing cells. 72.53% +/- 6.24 of DMSO vehicle control treated cells displayed blebbing
307 while only 15.6% +/- 6.28 of cells treated with GSK269962 (100 nM) displayed bleb
308 formation in response to 30 μM AYPGKF-NH_2 (Fig. 6A-C). To further confirm the role of
309 RhoA in PAR4-mediated changes in the plasma membrane, a RhoA knock out HEK-293
310 cell line (RhoA-KO HEK) was created by use of CRISPR/Cas9 targeting. RhoA-KO HEK
311 cells and control HEK-293 cells were transiently transfected with PAR4-YFP, stimulated
312 with 30 μM AYPGKF-NH_2 and imaged by confocal microscopy (Fig. 6D-F). 75% +/- 7.8
313 of control HEK-293 cells expressing PAR4-YFP and treated with AYPGKF-NH_2 displayed
314 membrane blebbing while RhoA-KO HEK expressing PAR4-YFP show significantly fewer
315 cells with blebs in response to agonist (22.8% +/- 6.2) (Fig. 6F). Taken together, these data
316 indicate that stimulation of PAR4-YFP elicits cell shape changes that are blocked by
317 blebbistatin and by the ROCK inhibitor GSK269962. Further, these cell shape changes do
318 not occur in cells that do not express RhoA protein, suggesting that this signalling pathway
319 is a RhoA and ROCK dependent pathway.
320
321 To confirm that these cellular responses can also be recapitulated by a physiological
322 PAR4 agonist, we tested the ability of thrombin to elicit similar cell shape changes. Since
323 thrombin can also activate PAR1 which is endogenously expressed in HEK-293 cells we
324 conducted these experiments in PAR1 knockout HEK-293 cells (PAR1-KO HEK) (Mihara
325 *et al.*, 2016) stably expressing PAR4-YFP (PAR1-KO-HEK-PAR4-YFP). PAR1-KO-HEK-
326 PAR4-YFP cells were treated with 3 U/ml thrombin and visualized by confocal
327 microscopy. Treatment of cells with thrombin caused cell shape changes similar to what
328 was observed in HEK-293-PAR4-YFP cells treated with AYPGKF-NH_2 (Fig. 7A). PAR1-
329 KO-HEK-PAR4-YFP cells were then treated with blebbistatin prior to thrombin

330 stimulation (Fig. 7B). Blebbistatin significantly reduced the number of PAR1-KO-HEK-
331 PAR4-YFP cells displaying membrane blebs from 68.3% +/- 4.6 to 11.67% +/- 5.78 (Fig.
332 7D). Finally, PAR1-KO-HEK-PAR4-YFP cells were treated with GSK269962 prior to
333 stimulation with thrombin (Fig. 7C). GSK269962 (100 nM) significantly reduced the
334 number of cells that displayed blebbing in response to thrombin stimulation (Fig. 7D).
335 Together these data indicates that cell blebbing is triggered not only by the synthetic PAR4
336 activating peptide AYPGKF-NH_2, but also by one of the endogenous activators of PAR4,
337 thrombin, in a PAR1 null background. Cell shape changes mediated by thrombin activation
338 of PAR4 are also RhoA- and ROCK-dependent.
339
340 **PAR4-mediated cell shape change is β-arrestin dependent**
341 Since the non-blebbing dRS-PAR4-YFP expressing cells are also deficient in β-
342 arrestin recruitment (Ramachandran *et al.*, 2017), we next examined the contribution of β-
343 arrestin-mediated signalling in PAR4-dependent cell membrane blebbing. To elucidate a
344 role for β-arrestins in PAR4-mediated cell shape change, a β-arrestin-1 and -2 double
345 knockout cell line (β-arrestin-1/-2 KO HEK) was created using CRISPR/Cas9 targeting. β-
346 arrestin-1/-2 KO HEK cells transiently expressing PAR4-YFP (β-arrestin-1/-2 KO HEK-
347 PAR4-YFP) were treated with 30 μM AYPGKF-NH_2 and visualized by confocal
348 microscopy. A significant reduction in the number of blebbing β-arrestin-1/-2 KO HEK-
349 PAR4-YFP (46%+/-8.2) was observed when compared to control HEK-293 cells
350 transiently expressing PAR4-YFP (80.8%+/- 6.1)(Fig. 8A-C).
351
352 Since recent reports have questioned whether β-arrestin mediated signalling can
353 occur in the absence of G-protein activation (Grundmann *et al.*, 2018) we sought to
354 understand this requirement in the context of PAR4 signalling. Even though $G\alpha_{q/11}$ and $G\alpha_i$
355 recruitment was not implicated in PAR4 dependent membrane blebbing, we nevertheless
356 examined the effect of blocking these pathways on β-arrestin-1/-2 recruitment to PAR4. To
357 this end we blocked $G\alpha_{q/11}$ with the inhibitor YM-254890 (100 nM) and blocked $G\alpha_i$ with
358 pertussis toxin (100 nM) and examined their ability to disrupt β-arrestin recruitment to
359 PAR4-YFP. We employed a BRET assay to monitor interaction between PAR4-YFP and
360 β-arrestin-1-Rluc or β-arrestin 2-Rluc in response to 30, 100 and 300 μM AYPGKF-NH_2.
361 Treatment of cells with YM-254890 did not significantly reduce recruitment of β-arrestin-1
362 or β-arrestin-2 recruitment to PAR4 at 30 μM or 100 μM concentrations of AYPGKF-NH_2
363 but did significanctly reduce recruitment of both β-arrestin-1 and -2 at the 300 μM
364 AYPGKF-NH_2 (Fig. 8D) treatment condition. Treatment of cells with pertussis toxin had
365 no effect on β-arrestin recruitment at any of the concentration tested (Fig. 8E).
366
367 Finally, we tested a role for Gβγ signalling in PAR4-mediated cell shape change
368 using the Gβγ inhibitor gallein (10 μM). HEK-293 cells stably expressing PAR4-YFP were
369 incubated with gallein or DMSO vehicle control prior to treatment with 30 μM AYPGKF-
370 NH_2. Cells treated with gallein did not show a significant reduction in membrane blebbing
371 compared to DMSO treated cells, 61.75% +/- 4.5 and 85.28% +/- 5.2 (Fig. 9A-C). Cells
372 expressing PAR4-YFP and either β-arrestin-1-Rluc or -2-Rluc incubated with gallein prior
373 to treatment with AYPGKF-NH_2 at 30, 100 and 300 μM also retained their ability to recruit
374 β-arrestin-1 and -2 at all concentrations of AYPGKF-NH_2 (Fig. 9D). Taken together these

375 data show that PAR4-mediated cell shape changes is independent of $G\alpha_{q/11}$, $G\alpha_i$ and $G\beta\gamma$.
376 Further inhibition of $G\alpha_i$ and $G\beta\gamma$ individually does not impede β-arrestin recruitment to
377 PAR4, while $G\alpha_{q/11}$ inhibition partially reduces β-arrestin recruitment to PAR4.
378
379 **PAR4 activation in rat primary aortic vascular smooth muscle cells leads to cell shape**
380 **changes.**
381 In order to examine whether PAR4 activation triggered cell blebbing in cells that
382 endogenously express PAR4, we turned to the rat vascular smooth muscle cells. Vascular
383 smooth muscle cells are reported to express PAR4 (Bretschneider *et al.*, 2001; Dangwal *et*
384 *al.*, 2011) and in our hands rat aortic smooth muscle cells from both WKY and SHR rats
385 expressed PAR4 (Fig. 10I). We labelled the smooth muscle cell membrane with cell mask
386 (ThermoFisher) and stimulated with 30 μM AYPGKF-NH_2. Both WKY and SHR VSMC
387 displayed cell shape changes resembling membrane blebs in response to PAR4 agonist
388 treatment (Fig 10A, E). In order to establish whether the signalling mechanism for these
389 cell shape changes was the same in both VSMC and HEK-293 cells, we pretreated VSMC
390 with blebbistatin and the ROCK inhibitor GSK269962 prior to activating PAR4 with 30
391 μM AYPGKF-NH_2. 67.25 +/- 6.6% of WKY cells display cell shape changes in response
392 to PAR4 agonist, (Fig. 10A), which was significantly reduced with treatment blebbistatin
393 (9.0 +/- 3.1%) and with treatment with GSK269962 (6.5 +/- 0.28%) (Fig. 10B-D).
394 Consistent with these findings, 65.75 +/- 5.4% of SHR cells also displayed blebbing
395 following PAR4 activation and these responses were significantly reduced with blebbistatin
396 (14.5 +/- 1.9%) and with GSK269962, (15.5 +/- 3.1%) treatment (Fig. 10F-H). These data
397 indicate that endogenous PAR4 activation elicits membrane blebbing in VSMC that is
398 ROCK dependent in keeping with our findings in the HEK-293 cells exogenously
399 expressing PAR4.
400
401 **PAR4 mediated β-arrestin recruitment influences gene transcription.**
402 β-arrestins are scaffold proteins that couple GPCRs to multiple signalling cascades
403 in a manner that is differential to heterotrimeric G-protein coupling (Laporte and Scott,
404 2019). Since PAR4-mediated membrane blebbing is β-arrestin-dependent, we sought to
405 take a complementary approach to explore PAR4-mediated β-arrestin-dependent pathways.
406 In order to do this, we compared the transcriptomes of HEK-293 and β-arrestin-1/-2-KO
407 HEK cells activated with 30 μM AYPGKF-NH_2 for 3 hours as well as the transcriptomes
408 of untreated HEK-293 and β-arrestin-1/-2-KO HEK cells transiently expressing PAR4-
409 YFP. Principal component analysis and hierarchical clustering of gene expression profiles
410 shows clear clustering of HEK-293 samples as well as treated and untreated β-arrestin-1/-2-
411 KO HEK samples (Fig. S1A-D). Differential expression analysis between the HEK-293
412 cells and β-arrestin-1/-2-KO HEK cells yielded 2,764 and 3,155 significantly differentially
413 expressed genes (P_{adj} <0.05 and Fold-Change>2) between the HEK-293 and β-arrestin-1/-
414 2-KO HEK samples in untreated and treated conditions, respectively. A total of 1,313
415 differentially expressed genes were shared between the untreated and treated conditions
416 (Fig. 11). Of note, even though we see a depletion of β-arrestin protein in our β-arrestin-1/-
417 2-KO HEK cell line, we do not see down regulation of β-arrestin-1 or -2 transcripts in the
418 RNA seq profile. Gene ontology (GO) enrichment analysis of the significantly upregulated
419 genes in samples treated with 30 μM AYPGKF-NH_2 (n = 1506) revealed biological process

terms related to cell-cell adhesion, and G-protein coupled receptor signalling pathway which are consistent with our finding of membrane blebbing triggered by PAR4 activation. (Table 1). Additionally, GO terms relating to known functions of PAR4 including neuron-neuron synaptic transmission, blood coagulation, blood circulation, and sensory perception were also found to be enriched in upregulated genes (Table 1). GO analysis of the downregulated genes (Treated only: n = 336) revealed biological process terms related to intracellular signal transduction. (Table 2). Taken together, these results suggest that β-arrestin-1/-2 are important regulators of signalling and gene transcription following PAR4 activation. Genes upregulated relating to cell-cell adhesion and GPCR signalling are consistent with our finding of β-arrestin-dependent membrane blebbing following PAR4 activation.

Discussion

We have demonstrated that activation of PAR4 with thrombin or the synthetic PAR4 activating peptide, AYPGKF-NH_2, causes a rapid cell shape change response in PAR4-transfected HEK-293 cells or in vascular smooth muscle cells that endogenously express PAR4. Cell shape changes are pharmacologically inhibited by blebbistatin and are consistent with membrane bleb formation. We observed membrane blebs that formed within 2-5 minutes of agonist treatment and lasted for upto 30 minutes. Membrane blebbing could be pharmacologically inhibited by the ROCK inhibitor GSK269962 or through CRISPR/Cas9 mediated knockout of RhoA. CRISPR/Cas9 knockout of β-arrestin-1 and -2 partially abolished PAR4-dependent mebrane blebbing. We further found PAR4-dependent membrane bleb formation to be independent of $G\alpha_{q/11}$, $G\alpha_{i,}$ $G\beta\gamma$, and PKC. Overall, our data suggest that RhoA-dependent membrane blebbing occurs downstream of PAR4 activation and β-arrestin recruitment.

Non-apoptotic cell membrane blebbing plays an important role in various physiological and pathologlical processes. Various stimuli have been reported to trigger bleb formation leading to cellular responses including enhanced cell motility, invasion, cell locomotion, and regulation of cell polarity in embryonic development (Charras and Paluch, 2008; Fackler and Grosse, 2008; Ikenouchi and Aoki, 2016). Blebbing is also an important regulator of wound healing, immune cell maturation, and inflammation. In this context, the PAR family of GPCRs is well established as critical regulators of the innate immune response to injury and infection. PARs also elicit cellular responses that allow coagulation cascade enzymes such as thrombin and other serine proteinases to regulate various cellular functions. PAR1 and PAR4 serve as the receptors for thrombin on human platelets, though these receptors regulate different aspects of platelet activation (Coughlin, 1999; Kahn *et al.*, 1999; Ma *et al.*, 2005; Holinstat *et al.*, 2006; Voss *et al.*, 2007). PAR4 is described as the low-affinity thrombin receptor on human platelets. This lower affinity stems from the lack of a hirudin like binding site for thrombin on PAR4, that is present on PAR1. In platelets, PAR4 activation typically requires a much higher concentration of thrombin to be present and PAR4 activation typically results in more sustained calcium signalling compared to PAR1-dependent signalling (Covic *et al.*, 2000; Shapiro *et al.*, 2000).

Both PAR1 and PAR4 activation triggers platelet aggregation, with PAR4 signalling critical for full platelet spreading and formation of stable aggregates. In rodents,

466 PAR4 serves as the sole thrombin receptor in platelets (Sambrano *et al.*, 2001). It has been
467 previously shown in $G\alpha_{q/11}$ knock out mice, that a thrombin activated $G\alpha_{q/11}$-mediated
468 scalcium response is necessary for platelet aggregation (Offermanns *et al.*, 1997). However,
469 platelets from the mouse $G\alpha_{q/11}$ knockout retained the ability to change shape in response to
470 thrombin stimulation. Similar findings were reported in platelets treated with a small
471 molecule $G\alpha_{q/11}$ antagonist UBO-QIC showing that platelet aggregation was inhibited
472 without affecting shape change responses (Inamdar *et al.*, 2015). Consistent with these
473 findings, we have observed a cell shape change specific to PAR4 activation that is $G_{q/11}$-
474 independent and a RhoA-mediated phenomenon. Recent evidence suggests that PAR4
475 plays an important role in promoting platelet granule release and platelet-leukocyte
476 interactions (Rigg *et al.*, 2019), responses which also rely on a RhoA-mediated cytoskeletal
477 rearrangement (Moers *et al.*, 2003; Aslan and Mccarty, 2013). These findings raise the
478 interesting possibility that different signalling pathways may underlie PAR4 regulation of
479 distinct aspects of platelet activation and further study is required to fully elucidate the role
480 of different signalling cascades in mediating PAR4 responses in platelets. Our studies
481 suggest that in HEK cells the $G\alpha_{q/11}$-coupled pathway and the RhoA pathway, which in this
482 instance is likely downstream of $G\alpha_{12/13}$ coupling, can act independently and therefore may
483 be independent targets for pharmacological manipulation.
484
485 PAR4 expression has also been reported in other cell types involved in the response
486 to injury including endothelial cells and smooth muscle cells (Bretschneider *et al.*, 2001;
487 Hamilton *et al.*, 2001; Fujiwara *et al.*, 2005; Ritchie *et al.*, 2007). Here we demonstrate that
488 agonist stimulation of endogenous PAR4 in vascular smooth muscle cells leads to
489 membrane blebbing. This finding is consistent with a previous study which showed that
490 another GPCR AT1R mediates membrane blebbing by a RhoA-dependent mechanism in a
491 vascular smooth muscle cell line (Godin and Ferguson, 2010). RhoA is well established as
492 a mediator of changes in the plasma membrane actin cytoskeleton and in regulating GPCR
493 mediated cell shape change (Barnes *et al.*, 2005; Godin and Ferguson, 2010; Aoki *et al.*,
494 2016). Our findings add PAR4-dependent signalling to the cell surface signalling molecules
495 that can trigger this pathway.
496
497 β-arrestins are now well established as important molecular scaffolds linking
498 GPCRs to not only molecular endocytic partners to facilitate receptor endocytosis, but also
499 to second messenger signal cascades (Ferguson, 2001; Magalhaes *et al.*, 2012). For
500 example β-arrestins link GPCRs to p44/42 MAP kinase signalling from the endosome
501 (Luttrell *et al.*, 2001; Luttrell and Lefkowitz, 2002). PAR4 couples to both β-arrestin-1 and
502 β-arrestin-2 and PAR4-mediated phosphorylation of AKT in platelets is β-arrestin-2-
503 dependent (Li *et al.*, 2011). We explored β-arrestin-1/-2-dependent PAR4 signalling by
504 using RNA sequencing analysis in HEK cells and β-arrestin knock out HEK cells treated or
505 not with the PAR4 specific agonist peptide AYPGKF-NH_2. Our data shows that β-arrestins
506 can regulate PAR4-dependent gene transcription. Consistent with our finding that PAR4
507 mediates membrane bleb formation, we see an upregulation of gene ontology terms in cell-
508 cell adhesion, blood coagulation and blood circulation. It is well established that PAR4
509 activation regulates platelet response, thus links to gene ontology terms related to blood
510 coagulation are perhaps unsurprising and uncover an important link to β-arrestin in these
511 processes. Our RNA-seq analysis uncovered a number of other additional signalling

512 pathways that could be linked to PAR4 and β-arrestin such as neuron-neuron synaptic
513 transmission (GO:0007270), natural killer cell activation (GO:0030101) and sensory
514 perception (GO:0007600). PAR4 expression has been reported in various neuronal and
515 immune cells and these data provide impetus to further examine the roles of PAR4 in these
516 cells (Henrich-Noack *et al.*, 2006; Russell *et al.*, 2009; Peng *et al.*, 2019). More broadly
517 were also interested in understanding if PAR4 signalling to β-arrestin could proceed
518 independently of G-protein coupling. Blocking $G\alpha_{q/11}$ partially inhibited β-arrestin
519 recruitment to PAR4 while blocking of $G\alpha_{i}$- or βγ-mediated signalling had no effect. It
520 however remains to be determined whether β-arrestin recruitment dependent signalling
521 downstream of PAR4 is truly independent of G-protein coupling or occurs following
522 $G\alpha_{12/13}$ activation.
523
524 In conclusion, we have uncovered a PAR4-mediated cellular response that is
525 independent of $G\alpha_{q/11}$ coupling and occurs downstream of RhoA activation and β-arrestin
526 signalling. These data provide further evidence for pathway-selective signalling responses
527 through PAR4 and may guide future development of PAR4 targeting strategies.

528 **Figure Legends:**
529
530 **Figure 1. Activation PAR4 mediates a cell shape change response.** Representative
531 confocal micrographs, showing HEK-293 cell stably expressing PAR4-YFP (A, B) Cells
532 were treated with 30 μM AYPGKF-NH_2 for 2 minutes prior to imaging. Size bars are 20
533 μm, arrows show cell shape change. HEK-293 cells stably expressing PAR4-YFP (C-E)
534 were incubated in either DMSO (C) or 10 μM blebbistatin (B) for 15 minutes prior to a 2-
535 minute treatment with 30 μM AYPGKF-NH_2 followed by confocal microscopy. Arrows
536 show bleb formation, size bars are 20 μm. (E) graph shows mean +/- SEM, n = 4, asterisk
537 shows significantly different, Mann-Whitney, $p<0.05$.
538
539 **Figure 2. Activation PAR4 mediates a cell shape change response is dependent on an 8**
540 **amino acid sequence.**
541 HEK-293 transiently expressing dRS-PAR4-YFP (A-C) were treated with 30 μM
542 AYPGKF-NH_2 for 2 minutes prior to imaging and scored for cell shape change or no
543 change, graph shows mean +/- SEM, size bars are 20 μm, asterisks indicates statistically
544 significant, t-test, n = 3, $p<0.005$.
545
546 **Figure 3. PAR4-mediated cell shape change is $G\alpha_{q/11}$-independent.** HEK-293 cells
547 transiently expressing PAR4-mCherry (not shown) with PKCβ1-GFP, were treated with
548 DMSO followed by stimulation with 30 μM AYPGKF-NH_2 (A-C) or with 100 nM
549 YM254890 for 20 minutes followed by stimulation with 30 μM AYPGKF-NH_2 (D-F).
550 Arrows show bleb formation, size bars are 20 μm. Graph shows mean +/- SEM, n = 3, not
551 significantly different, t-test (G).
552
553 **Figure 4. PAR4-mediated cell shape change is PKC-independent.** HEK-293 cells
554 transiently expressing either PAR4-mCherry (not shown) (A, B) or dRS-PAR4-mCherry
555 (not shown) (C, D) with PKCβ1-GFP, were treated with 30 μM AYPGKF-NH_2 and imaged
556 by confocal microscopy, size bars are 20 μm. HEK-293 cells stably expressing PAR4-YFP
557 were incubated with DMSO (E) or with 100 nM GO6983 for 15 minutes (F) prior to 2 a
558 minute stimulation with 30 μM AYPGKF-NH_2 and subsequent imaging by confocal
559 microscopy. Cells were scored for blebbing or non-blebbing, graph shows mean +/- SEM,
560 n = 4, not significantly different, t-test (G).
561
562 **Figure 5. PAR4-mediated cell shape change is $G\alpha_i$-independent.** HEK-293 cells stably
563 expressing PAR4-YFP were incubated in either DMSO (A) or 100 nM PTX (B) for 18
564 hours prior to 30 μM AYPGKF-NH_2 treatment for 2 minutes and confocal imaging.
565 Arrows show bleb formation, size bars are 20 μm. Graphs shows mean +/- SEM, n = 3, not
566 significantly different, Mann-Whitney (C).
567
568 **Figure 6. PAR4-mediated cell shape change is RhoA- and ROCK-dependent.** HEK-
569 293 cells stably expressing PAR4-YFP were incubated in either DMSO (A) or 100 nM
570 GSK269962 for 1 hour (B) prior to a 2 minute treatment with 30 μM AYPGKF-NH_2
571 followed by confocal microscopy. Arrows show bleb formation, size bars are 20 μm. (C)
572 graph shows mean +/- SEM, n = 4, asterisk shows significantly different, Mann-Whitney,

573 p<0.05. HEK-293 cells and RhoA-KO HEK transiently expressing PAR4-YFP were
574 stimulated with 30 μM AYPGKF-NH_2 for 2 minutes prior to confocal imaging (D, E). (F)
575 Graph shows mean +/- SEM, n = 4, asterisk shows significantly different, Mann-Whitney,
576 p<0.05.
577
578 **Figure 7. Thrombin-induced PAR4-mediated cell shape change is ROCK-dependent.**
579 PAR1-KO-PAR4-YFP-HEK-293 cells were incubated in either DMSO (A) or 10 μM
580 blebbistatin for 15 minutes (B) or 100 nM GSK269962 for 1 hour (C) prior to a 2 minute
581 treatment with 30 μM AYPGKF-NH_2 followed by confocal microscopy. Arrows show bleb
582 formation, size bars are 20 μm. Graph shows mean +/- SEM, n = 4, asterisk shows
583 significantly different, Mann-Whitney, p<0.05 (D).
584
585 **Figure 8. PAR4-mediated cell shape change is β-arrestin-dependent.** HEK-293 cells
586 (A) or β-arrestin-1/-2-KO HEK transiently expressing PAR4-YFP (B) were stimulated in
587 30 μM AYPGKF-NH_2 for 2 minutes prior to confocal imaging. Arrows show bleb
588 formation, size bars are 20 μm. (C) Graph shows mean +/- SEM, n=3, asterisk shows
589 significantly different, t-test, P<0.05). HEK-293 cells transiently expressing PAR4-YFP
590 with either β-arrestin-1-Rluc or -2-Rluc were incubated in DMSO or 100 nM YM254890
591 (D) or 100 nM PTX for 18 hours (E) for 20 minutes prior to testing in the BRET assay.
592 Graph shows mean +/- SEM, n = 4, asterisk shows significantly different, 2-way ANOVA.
593
594 **Figure 9. PAR4-mediated cell shape change is $G_{\beta\gamma}$-independent.** HEK-293 cells stably
595 expressing PAR4-YFP were incubated in either DMSO (A) or 10 μM gallein for 20
596 minutes prior to 30 μM AYPGKF-NH_2 for 2 minutes and confocal imaging. Arrows show
597 bleb formation, size bars are 20 μm. Graphs shows mean +/- SEM, n=4, not significantly
598 different, Mann-Whitney (C). HEK-293 cells transiently expressing PAR4-YFP with either
599 β-arrestin 1-Rluc or -2-Rluc were incubated in DMSO or with 10 μM gallein for 20
600 minutes (H) prior to testing in the BRET assay. Graph shows, mean +/- SEM, n = 4, not
601 significantly different 2-way ANOVA.
602
603 **Figure 10. PAR4 mediates membrane blebs in vascular smooth muscle cells.** Primary
604 cultured vascular smooth muscle cells derived from Wistar Kyoto (WKY) (A-D) or from
605 spontaneously hypertensive (SHR) (E-H) rats were pre-incubated for 10 minutes in cell
606 mask to stain the plasma membrane, cells were then treated with 30 μM AYPGFK-NH_2
607 and imaged by confocal microscopy. WKY cells and SHR cells were preincubated with
608 blebbistatin or with GSK269962 prior to stimulation with AYPGFK-NH_2 (B, C, F, G),
609 arrows show bleb formation, size bars are 20 μm. Images were scored for blebbing or
610 non-blebbing (D and H), graph shows mean +/- SEM, n = 4, asterisk shows significantly
611 different, ANOVA, p<0.001.
612
613 **Table 1: Differential PAR4-mediated gene regulation in β-arrestin-1/-2 knock out**
614 **cells.**
615 Gene ontology (GO) biological process terms for genes upregulated (A) and downregulated
616 (B) genes in β-arrestin-1/-2-KO HEK cells transiently expressing PAR4-YFP treated with
617 30 μM AYPGKF-NH_2 for 3 hours compared to HEK-293 cells under the same conditions.

618 Top ten significant terms ($p<0.05$) where the highest enrichment for biological process are
619 presented. Terms related to the membrane blebbing phenotype are in bold and terms related
620 to known functions of PAR4 are italicized.
621
622 **Supplementary Figure 1. CRISPR/Cas9 knock out of β-arrestin-1/-2 and RhoA in**
623 **HEK-293 cells.**
624 HEK-293 cells were transiently transfected with either guide RNA specific to β-arrestin-1
625 and β-arrestin-2, or four guide RNAs specific to RhoA. Cells expressing pSpCas9(BB)-
626 2A-GFP encoding guide RNAs were selected for using FACS Aria cell sorter and
627 subsequently knockout was determined by western blot.
628
629 **Supplementary Figure 2. Knockout of β-arrestin-1/-2 results in differentially**
630 **expressed genes. (A)**Principal component analysis biplot showing the first two principal
631 components (PCs) that account for most of the variance between samples. **(B)** Venn
632 diagram showing overlap of differentially expressed genes ($P_{adj}<0.05$ and Fold-Change>2)
633 in β-arrestin-1/-2-KO HEK cells treated with PAR4 agonist (Treated) or with vehicle
634 (Untreated) when compared to similarly treated HEK-293 cells. **(C & D)** Volcano plots
635 showing significantly differentially expressed genes between β-arrestin-1/-2-KO and HEK-
636 293 cells when treated with vehicle **(C)** or 30 μM AYPGKF-NH_2 **(D)**. Of the differentially
637 expressed genes, 666 were downregulated and unique to untreated cells, 336 were
638 downregulated and unique to treated cells, and 636 were found to be downregulated in both
639 conditions. Additionally, 785 genes were upregulated and unique to untreated cells, 1506
640 were upregulated and unique to treated cells, and 667 were found to be upregulated in both
641 conditions.

642 **References:**

643 Anders S, Pyl PT, and Huber W (2015) HTSeq--a Python framework to work with high-
644 throughput sequencing data. *Bioinforma Oxf Engl* **31**:166–169.

645 Anthony DF, Sin YY, Vadrevu S, Advant N, Day JP, Byrne AM, Lynch MJ, Milligan G,
646 Houslay MD, and Baillie GS (2011) β-Arrestin 1 inhibits the GTPase-activating
647 protein function of ARHGAP21, promoting activation of RhoA following
648 angiotensin II type 1A receptor stimulation. *Mol Cell Biol* **31**:1066–1075.

649 Aoki K, Maeda F, Nagasako T, Mochizuki Y, Uchida S, and Ikenouchi J (2016) A RhoA
650 and Rnd3 cycle regulates actin reassembly during membrane blebbing. *Proc Natl*
651 *Acad Sci U S A* **113**:E1863-1871.

652 Aslan JE, and Mccarty OJT (2013) Rho GTPases in platelet function. *J Thromb Haemost*
653 **11**:35–46.

654 Barnes WG, Reiter E, Violin JD, Ren XR, Milligan G, and Lefkowitz RJ (2005) beta-
655 Arrestin 1 and Galphaq/11 coordinately activate RhoA and stress fiber formation
656 following receptor stimulation. *J Biol Chem* **280**:8041–8050.

657 Bretschneider E, Kaufmann R, Braun M, Nowak G, Glusa E, and Schror K (2001)
658 Evidence for functionally active protease-activated receptor-4 (PAR-4) in human
659 vascular smooth muscle cells. *Br J Pharmacol* **132**:1441–1446.

660 Charras G, and Paluch E (2008) Blebs lead the way: how to migrate without lamellipodia.
661 *Nat Rev Mol Cell Biol* **9**:730–736.

662 CHARRAS GT (2008) A short history of blebbing. *J Microsc* **231**:466–478.

663 Charras GT, Coughlin M, Mitchison TJ, and Mahadevan L (2008) Life and Times of a
664 Cellular Bleb. *Biophys J* **94**:1836–1853.

665 Chen P, Douglas SD, Meshki J, and Tuluc F (2012) Neurokinin 1 receptor mediates
666 membrane blebbing and sheer stress-induced microparticle formation in HEK293
667 cells. *PloS One* **7**:e45322.

668 Cheung A, Dantzig JA, Hollingworth S, Baylor SM, Goldman YE, Mitchison TJ, and
669 Straight AF (2002) A small-molecule inhibitor of skeletal muscle myosin II. *Nat*
670 *Cell Biol* **4**:83–88.

671 Coughlin SR (1999) How the protease thrombin talks to cells. *Proc Natl Acad Sci U S A*
672 **96**:11023–11027.

673 Covic L, Gresser AL, and Kuliopulos A (2000) Biphasic kinetics of activation and
674 signaling for PAR1 and PAR4 thrombin receptors in platelets. *Biochemistry*
675 **39**:5458–5467.

676 Dale LB, Babwah AV, Bhattacharya M, Kelvin DJ, and Ferguson SS (2001) Spatial-
677 temporal patterning of metabotropic glutamate receptor-mediated inositol 1,4,5-
678 triphosphate, calcium, and protein kinase C oscillations: protein kinase C-dependent
679 receptor phosphorylation is not required. *J Biol Chem* **276**:35900–35908.

680 Dangwal S, Rauch BH, Gensch T, Dai L, Bretschneider E, Vogelaar CF, Schrör K, and
681 Rosenkranz AC (2011) High glucose enhances thrombin responses via protease-
682 activated receptor-4 in human vascular smooth muscle cells. *Arterioscler Thromb*
683 *Vasc Biol* **31**:624–633.

684 Dobin A, Davis CA, Schlesinger F, Drenkow J, Zaleski C, Jha S, Batut P, Chaisson M, and
685 Gingeras TR (2013) STAR: ultrafast universal RNA-seq aligner. *Bioinformatics*
686 **29**:15–21.

687 Exton JH (1996) Regulation of phosphoinositide phospholipases by hormones,
688 neurotransmitters, and other agonists linked to G proteins. *Annu Rev Pharmacol*
689 *Toxicol* **36**:481–509.

690 Fackler OT, and Grosse R (2008) Cell motility through plasma membrane blebbing. *J Cell*
691 *Biol* **181**:879–884.

692 Ferguson SS (2001) Evolving concepts in G protein-coupled receptor endocytosis: the role
693 in receptor desensitization and signaling. *Pharmacol Rev* **53**:1–24.

694 Ferguson SSG, and Caron MG (2004) Green Fluorescent Protein-Tagged β-Arrestin
695 Translocation as a Measure of G Protein-Coupled Receptor Activation, in *G Protein*
696 *Signaling: Methods and Protocols* (Smrcka AV ed) pp 121–126, Humana Press,
697 Totowa, NJ.

698 Fujiwara M, Jin E, Ghazizadeh M, and Kawanami O (2005) Activation of PAR4 induces a
699 distinct actin fiber formation via p38 MAPK in human lung endothelial cells. *J*
700 *Histochem Cytochem* **53**:1121–1129.

701 Godin CM, and Ferguson SSG (2010) The angiotensin II type 1 receptor induces
702 membrane blebbing by coupling to Rho A, Rho kinase, and myosin light chain
703 kinase. *Mol Pharmacol* **77**:903–911.

704 Gong X, Didan Y, Lock JG, and Strömblad S (2018) KIF13A-regulated RhoB plasma
705 membrane localization governs membrane blebbing and blebby amoeboid cell
706 migration. *EMBO J* **37**.

707 Gros R, Ding Q, Chorazyczewski J, Pickering JG, Limbird LE, and Feldman RD (2006)
708 Adenylyl cyclase isoform-selective regulation of vascular smooth muscle
709 proliferation and cytoskeletal reorganization. *Circ Res* **99**:845–852.

710 Grundmann M, Merten N, Malfacini D, Inoue Asuka, Preis P, Simon K, Rüttiger N, Ziegler
711 N, Benkel T, Schmitt NK, Ishida S, Müller I, Reher R, Kawakami K, Inoue Ayumi,
712 Rick U, Kühl T, Imhof D, Aoki J, König GM, Hoffmann C, Gomeza J, Wess J, and

713 Kostenis E (2018) Lack of beta-arrestin signaling in the absence of active G
714 proteins. *Nat Commun* **9**:341.

715 Gschwendt M, Dieterich S, Rennecke J, Kittstein W, Mueller HJ, and Johannes FJ (1996)
716 Inhibition of protein kinase C mu by various inhibitors. Differentiation from protein
717 kinase c isoenzymes. *FEBS Lett* **392**:77–80.

718 Hagmann J, Burger MM, and Dagan D (1999) Regulation of plasma membrane blebbing by
719 the cytoskeleton. *J Cell Biochem* **73**:488–499.

720 Hamilton JR, Frauman AG, and Cocks TM (2001) Increased expression of protease-
721 activated receptor-2 (PAR2) and PAR4 in human coronary artery by inflammatory
722 stimuli unveils endothelium-dependent relaxations to PAR2 and PAR4 agonists.
723 *Circ Res* **89**:92–98.

724 Henrich-Noack P, Riek-Burchardt M, Baldauf K, Reiser G, and Reymann KG (2006) Focal
725 ischemia induces expression of protease-activated receptor1 (PAR1) and PAR3 on
726 microglia and enhances PAR4 labeling in the penumbra. *Brain Res* **1070**:232–241.

727 Holinstat M, Voss B, Bilodeau ML, McLaughlin JN, Cleator J, and Hamm HE (2006)
728 PAR4, but not PAR1, signals human platelet aggregation via Ca2+ mobilization and
729 synergistic P2Y12 receptor activation. *J Biol Chem* **281**:26665–26674.

730 Ikenouchi J, and Aoki K (2016) Membrane bleb: A seesaw game of two small GTPases. -
731 PubMed - NCBI. *Small GTPases* **8**:85–89.

732 Inamdar V, Patel A, Manne BK, Dangelmaier C, and Kunapuli SP (2015) Characterization
733 of UBO-QIC as a Gαq inhibitor in platelets. *Platelets* **26**:771–778.

734 Kahn ML, Nakanishi-Matsui M, Shapiro MJ, Ishihara H, and Coughlin SR (1999)
735 Protease-activated receptors 1 and 4 mediate activation of human platelets by
736 thrombin. *J Clin Invest* **103**:879–887.

737 Kim S, Jin J, and Kunapuli SP (2006) Relative contribution of G-protein-coupled pathways
738 to protease-activated receptor-mediated Akt phosphorylation in platelets. *Blood*
739 **107**:947–954.

740 Kovács M, Tóth J, Hetényi C, Málnási-Csizmadia A, and Sellers JR (2004) Mechanism of
741 blebbistatin inhibition of myosin II. *J Biol Chem* **279**:35557–35563.

742 Laporte SA, and Scott MGH (2019) β-Arrestins: Multitask Scaffolds Orchestrating the
743 Where and When in Cell Signalling. *Methods Mol Biol Clifton NJ* **1957**:9–55.

744 Laser-Azogui A, Diamant-Levi T, Israeli S, Roytman Y, and Tsarfaty I (2014) Met-induced
745 membrane blebbing leads to amoeboid cell motility and invasion. *Oncogene*
746 **33**:1788–1798.

747 Lawrenson ID, Wimmer-Kleikamp SH, Lock P, Schoenwaelder SM, Down M, Boyd AW,
748 Alewood PF, and Lackmann M (2002) Ephrin-A5 induces rounding, blebbing and
749 de-adhesion of EphA3-expressing 293T and melanoma cells by CrkII and Rho-
750 mediated signalling. *J Cell Sci* **115**:1059–1072.

751 Li D, D'Angelo L, Chavez M, and Woulfe DS (2011) Arrestin-2 Differentially Regulates
752 PAR4 and ADP Receptor Signaling in Platelets. *J Biol Chem* **286**:3805–3814.

753 Love MI, Huber W, and Anders S (2014) Moderated estimation of fold change and
754 dispersion for RNA-seq data with DESeq2. *Genome Biol* **15**:550.

755 Luttrell LM, and Lefkowitz RJ (2002) The role of beta-arrestins in the termination and
756 transduction of G-protein-coupled receptor signals. *J Cell Sci* **115**:455–465.

757 Luttrell LM, Roudabush FL, Choy EW, Miller WE, Field ME, Pierce KL, and Lefkowitz
758 RJ (2001) Activation and targeting of extracellular signal-regulated kinases by beta-
759 arrestin scaffolds. *Proc Natl Acad Sci* **98**:2449–2454.

760 Ma L, Perini R, McKnight W, Dicay M, Klein A, Hollenberg MD, and Wallace JL (2005)
761 Proteinase-activated receptors 1 and 4 counter-regulate endostatin and VEGF
762 release from human platelets. *Proc Natl Acad Sci U S A* **102**:216–220.

763 Magalhaes AC, Dunn H, and Ferguson SS (2012) Regulation of GPCR activity, trafficking
764 and localization by GPCR-interacting proteins. *Br J Pharmacol* **165**:1717–1736.

765 Mi H, Huang X, Muruganujan A, Tang H, Mills C, Kang D, and Thomas PD (2017)
766 PANTHER version 11: expanded annotation data from Gene Ontology and
767 Reactome pathways, and data analysis tool enhancements. *Nucleic Acids Res*
768 **45**:D183–D189.

769 Mihara K, Ramachandran R, Saifeddine M, Hansen KK, Renaux B, Polley D, Gibson S,
770 Vanderboor C, and Hollenberg MD (2016) Thrombin-Mediated Direct Activation
771 of Proteinase-Activated Receptor-2: Another Target for Thrombin Signaling. *Mol*
772 *Pharmacol* **89**:606–614.

773 Moers A, Nieswandt B, Massberg S, Wettschureck N, Gruner S, Konrad I, Schulte V,
774 Aktas B, Gratacap MP, Simon MI, Gawaz M, and Offermanns S (2003) G13 is an
775 essential mediator of platelet activation in hemostasis and thrombosis. *Nat Med*
776 **9**:1418–1422.

777 Morrow DA, Braunwald E, Bonaca MP, Ameriso SF, Dalby AJ, Fish MP, Fox KA, Lipka
778 LJ, Liu X, Nicolau JC, Ophuis AJ, Paolasso E, Scirica BM, Spinar J, Theroux P,
779 Wiviott SD, Strony J, and Murphy SA (2012) Vorapaxar in the secondary
780 prevention of atherothrombotic events. *N Engl J Med* **366**:1404–1413.

781 Offermanns S, Toombs CF, Hu Y-H, and Simon MI (1997) Defective platelet activation in
782 Gα q -deficient mice. *Nature* **389**:183.

783 Peng Q, Ratnasothy K, Boardman DA, Jacob J, Tung SL, McCluskey D, Smyth LA,
784 Lechler RI, Dorling A, and Lombardi G (2019) Protease Activated Receptor 4 as a
785 Novel Modulator of Regulatory T Cell Function. *Front Immunol* **10**.

786 Pinner S, and Sahai E (2008) PDK1 regulates cancer cell motility by antagonising
787 inhibition of ROCK1 by RhoE. *Nat Cell Biol* **10**:127–137.

788 Policha A, Daneshtalab N, Chen L, Dale LB, Altier C, Khosravani H, Thomas WG,
789 Zamponi GW, and Ferguson SSG (2006) Role of angiotensin II type 1A receptor
790 phosphorylation, phospholipase D, and extracellular calcium in isoform-specific
791 protein kinase C membrane translocation responses. *J Biol Chem* **281**:26340–26349.

792 Ramachandran R, Mihara K, Mathur M, Rochdi MD, Bouvier M, DeFea K, and Hollenberg
793 MD (2009) Agonist-biased signaling via proteinase activated receptor-2: differential
794 activation of calcium and mitogen-activated protein kinase pathways. *Mol*
795 *Pharmacol* **76**:791–801.

796 Ramachandran R, Mihara K, Thibeault P, Vanderboor CM, Petri B, Saifeddine M, Bouvier
797 M, and Hollenberg MD (2017) Targeting a Proteinase-Activated Receptor 4 (PAR4)
798 Carboxyl Terminal Motif to Regulate Platelet Function. *Mol Pharmacol* **91**:287–
799 295.

800 Ramachandran R, Noorbakhsh F, Defea K, and Hollenberg MD (2012) Targeting
801 proteinase-activated receptors: therapeutic potential and challenges. *Nat Rev Drug*
802 *Discov* **11**:69–86.

803 Rigg RA, Healy LD, Chu TT, Ngo ATP, Mitrugno A, Zilberman-Rudenko J, Aslan JE,
804 Hinds MT, Vecchiarelli LD, Morgan TK, Gruber A, Temple KJ, Lindsley CW,
805 Duvernay MT, Hamm HE, and McCarty OJT (2019) Protease-activated receptor 4
806 activity promotes platelet granule release and platelet-leukocyte interactions.
807 *Platelets* **30**:126–135.

808 Ritchie E, Saka M, Mackenzie C, Drummond R, Wheeler-Jones C, Kanke T, and Plevin R
809 (2007) Cytokine upregulation of proteinase-activated-receptors 2 and 4 expression
810 mediated by p38 MAP kinase and inhibitory kappa B kinase beta in human
811 endothelial cells. *Br J Pharmacol* **150**:1044–1054.

812 Russell FA, Veldhoen VE, Tchitchkan D, and McDougall JJ (2009) Proteinase-activated
813 receptor-4 (PAR4) activation leads to sensitization of rat joint primary afferents via
814 a bradykinin B2 receptor-dependent mechanism. *J Neurophysiol* **103**:155–163.

815 Sah VP, Seasholtz TM, Sagi SA, and Brown JH (2000) The role of Rho in G protein-
816 coupled receptor signal transduction. *Annu Rev Pharmacol Toxicol* **40**:459–489.

817 Sambrano GR, Weiss EJ, Zheng YW, Huang W, and Coughlin SR (2001) Role of thrombin
818 signalling in platelets in haemostasis and thrombosis. *Nature* **413**:74–78.

819 Schmieder R, and Edwards R (2011) Quality control and preprocessing of metagenomic
820 datasets. *Bioinformatics* **27**:863–864.

821 Shapiro MJ, Weiss EJ, Faruqi TR, and Coughlin SR (2000) Protease-activated receptors 1
822 and 4 are shut off with distinct kinetics after activation by thrombin. *J Biol Chem*
823 **275**:25216–25221.

824 Stavenger RA, Cui H, Dowdell SE, Franz RG, Gaitanopoulos DE, Goodman KB, Hilfiker
825 MA, Ivy RL, Leber JD, Marino Joseph P, Oh H-J, Viet AQ, Xu W, Ye G, Zhang D,
826 Zhao Y, Jolivette LJ, Head MS, Semus SF, Elkins PA, Kirkpatrick RB, Dul E,
827 Khandekar SS, Yi T, Jung DK, Wright LL, Smith GK, Behm DJ, Doe CP, Bentley
828 R, Chen ZX, Hu E, and Lee D (2007) Discovery of Aminofurazan-
829 azabenzimidazoles as Inhibitors of Rho-Kinase with High Kinase Selectivity and
830 Antihypertensive Activity. *J Med Chem* **50**:2–5.

831 Straight AF, Cheung A, Limouze J, Chen I, Westwood NJ, Sellers JR, and Mitchison TJ
832 (2003) Dissecting temporal and spatial control of cytokinesis with a myosin II
833 Inhibitor. *Science* **299**:1743–1747.

834 Taniguchi M, Suzumura K, Nagai K, Kawasaki T, Takasaki J, Sekiguchi M, Moritani Y,
835 Saito T, Hayashi K, Fujita S, Tsukamoto S, and Suzuki K (2004) YM-254890
836 analogues, novel cyclic depsipeptides with Gαq/11 inhibitory activity from
837 Chromobacterium sp. QS3666. *Bioorg Med Chem* **12**:3125–3133.

838 Tinevez J-Y, Schulze U, Salbreux G, Roensch J, Joanny J-F, and Paluch E (2009) Role of
839 cortical tension in bleb growth. *Proc Natl Acad Sci U S A* **106**:18581–18586.

840 Voss B, McLaughlin JN, Holinstat M, Zent R, and Hamm HE (2007) PAR1, but not PAR4,
841 activates human platelets through a Gi/o/phosphoinositide-3 kinase signaling axis.
842 *Mol Pharmacol* **71**:1399–1406.

843 Wettschureck N, and Offermanns S (2005) Mammalian G proteins and their cell type
844 specific functions. *Physiol Rev* **85**:1159–1204.

845 Wilson SJ, Ismat FA, Wang Z, Cerra M, Narayan H, Raftis J, Gray TJ, Connell S, Garonzik
846 S, Ma X, Yang J, and Newby DE (2017) PAR4 (Protease-Activated Receptor 4)
847 Antagonism With BMS-986120 Inhibits Human Ex Vivo Thrombus Formation.
848 *Arterioscler Thromb Vasc Biol* ATVBAHA.117.310104.

849 Wong PC, Seiffert D, Bird JE, Watson CA, Bostwick JS, Giancarli M, Allegretto N, Hua J,
850 Harden D, Guay J, Callejo M, Miller MM, Lawrence RM, Banville J, Guy J,
851 Maxwell BD, Priestley ES, Marinier A, Wexler RR, Bouvier M, Gordon DA,
852 Schumacher WA, and Yang J (2017) Blockade of protease-activated receptor-4
853 (PAR4) provides robust antithrombotic activity with low bleeding. *Sci Transl Med*
854 **9**:eaaf5294.

855 Woulfe DS (2005) REVIEW ARTICLES: Platelet G protein-coupled receptors in
856 hemostasis and thrombosis. *J Thromb Haemost* **3**:2193–2200.

857 Xu WF, Andersen H, Whitmore TE, Presnell SR, Yee DP, Ching A, Gilbert T, Davie EW,
858 and Foster DC (1998) Cloning and characterization of human protease-activated
859 receptor 4. *Proc Natl Acad Sci U S A* **95**:6642–6646.

860 Zhang D, LaFortune TA, Krishnamurthy S, Esteva FJ, Cristofanilli M, Liu P, Lucci A,
861 Singh B, Hung M-C, Hortobagyi GN, and Ueno NT (2009) Epidermal growth factor
862 receptor tyrosine kinase inhibitor reverses mesenchymal to epithelial phenotype and
863 inhibits metastasis in inflammatory breast cancer. *Clin Cancer Res Off J Am Assoc*
864 *Cancer Res* **15**:6639–6648.

865

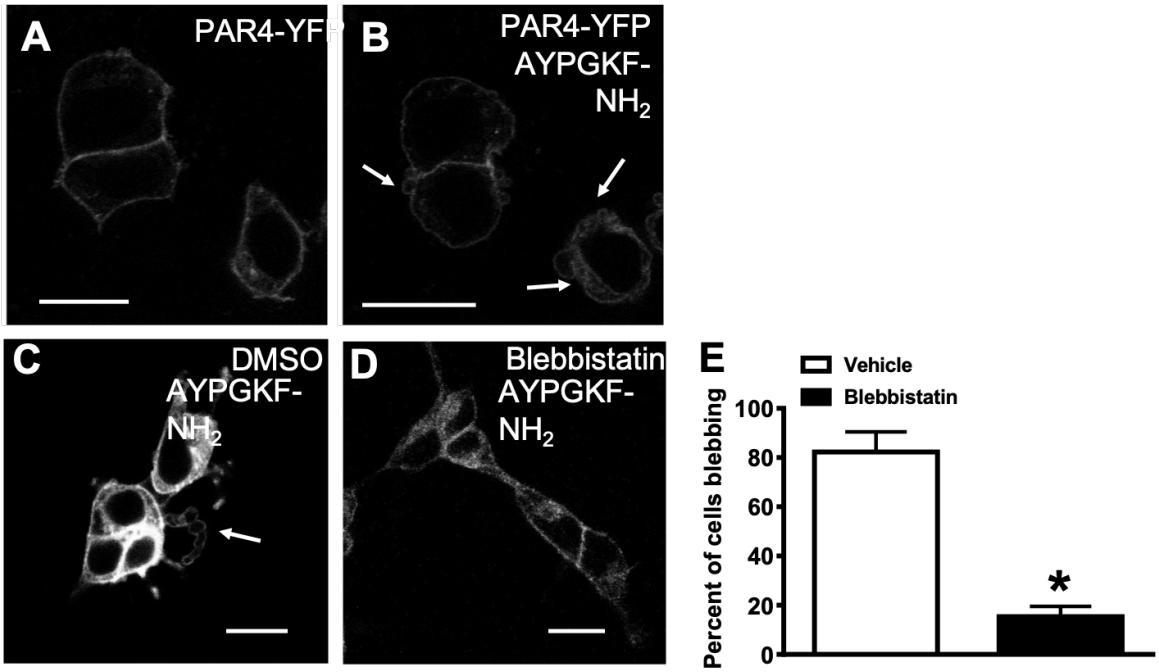
A
PAR4-YFP
B
PAR4-YFP
AYPGKF-
NH2
C
DMSO
AYPGKF-
NH2
D
Blebbistatin
AYPGKF-
NH2
E
Vehicle
Blebbistatin
Percent of cells blebbing
100
80
60
40
20
0
*

Figure 1

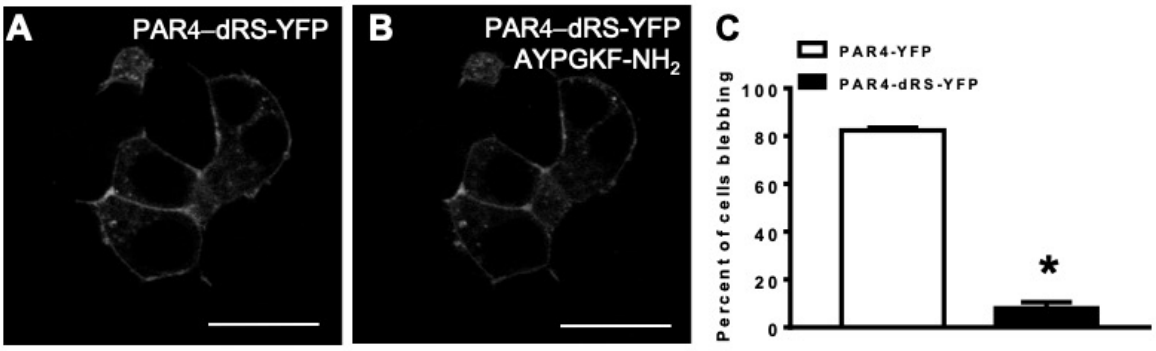
A
PAR4–dRS-YFP
B
PAR4–dRS-YFP
AYPGKF-NH2
C
PAR4-YFP
PAR4-dRS-YFP
Percent of cells blebbing
100
80
60
40
20
0
*

Figure 2

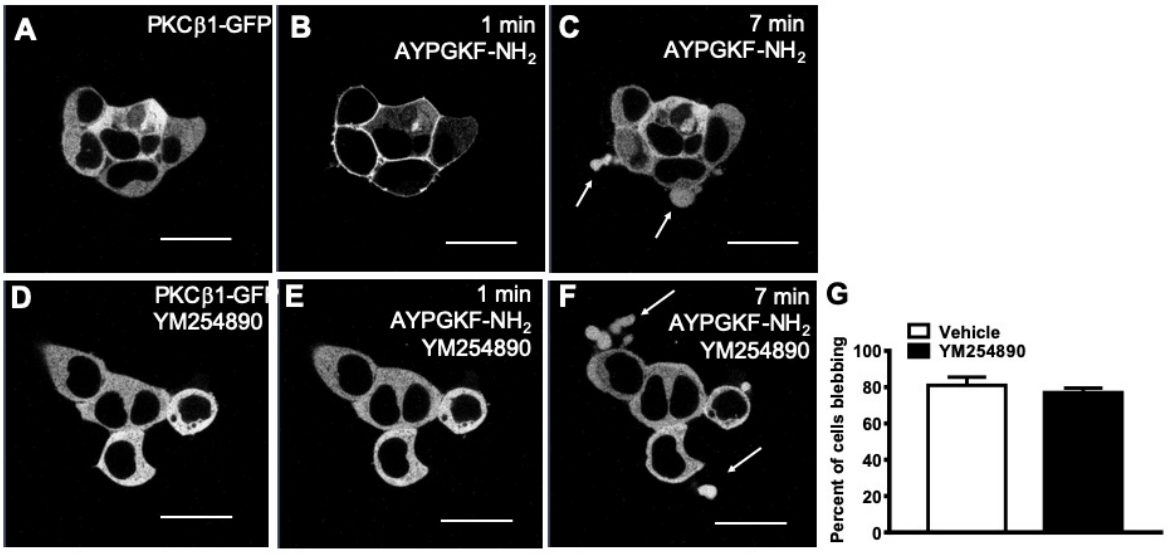

870

871 **Figure 3**

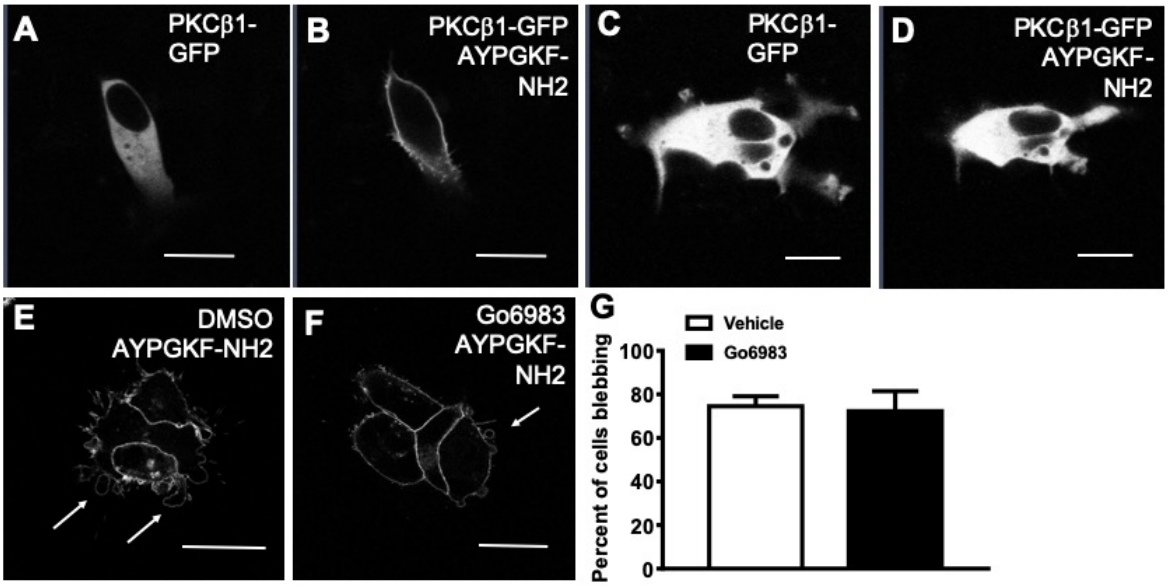

872

873 **Figure 4**

874

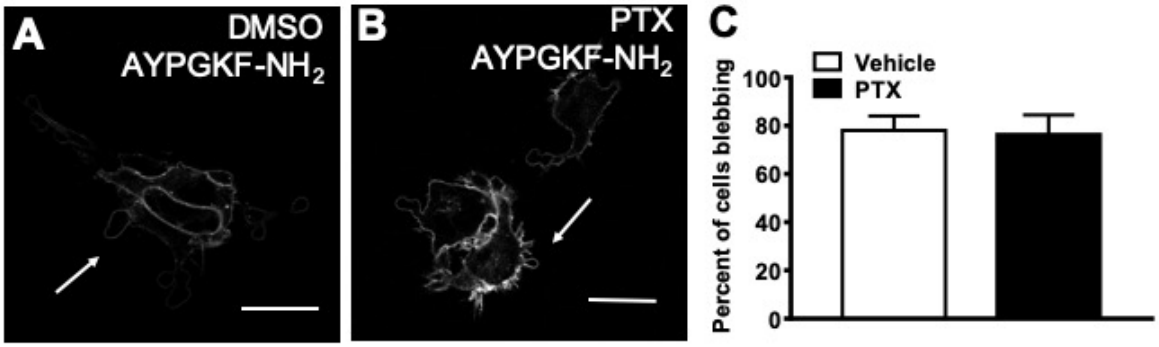

875 **Figure 5**

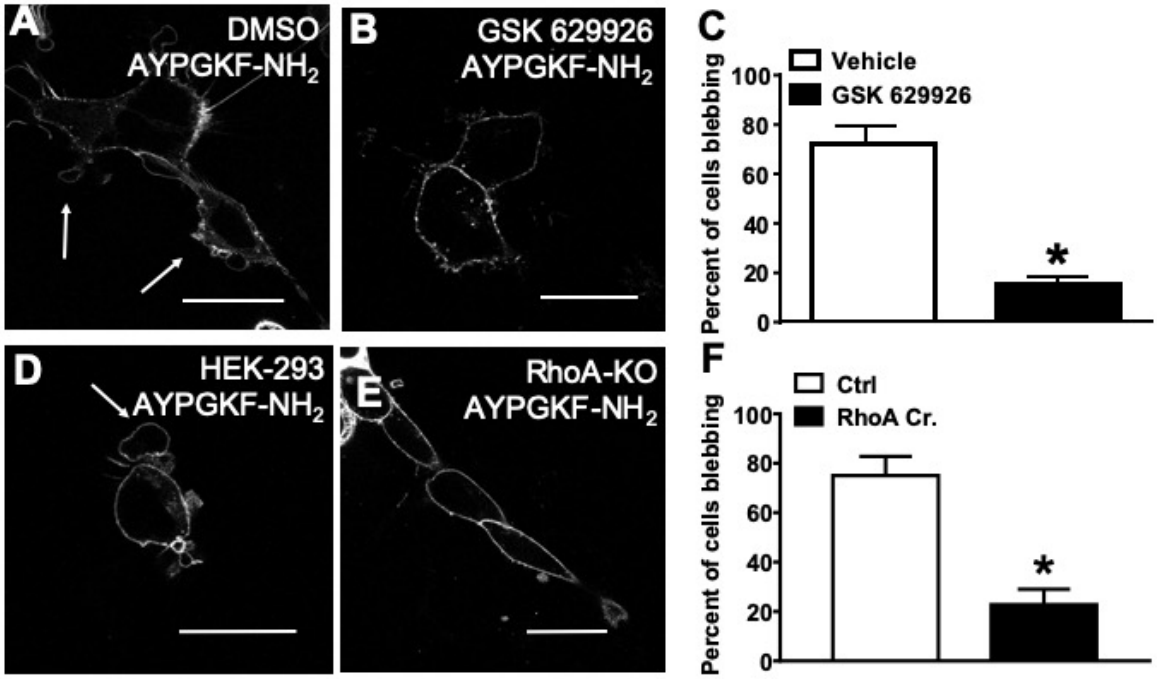
A
DMSO
AYPGKF-NH2
B
GSK 629926
AYPGKF-NH2
C
Vehicle
GSK 629926
Percent of cells blebbing
100
80
60
40
20
0
*
D
HEK-293
AYPGKF-NH2
E
RhoA-KO
AYPGKF-NH2
F
Ctrl
RhoA Cr.
Percent of cells blebbing
100
80
60
40
20
0
*

Figure 6

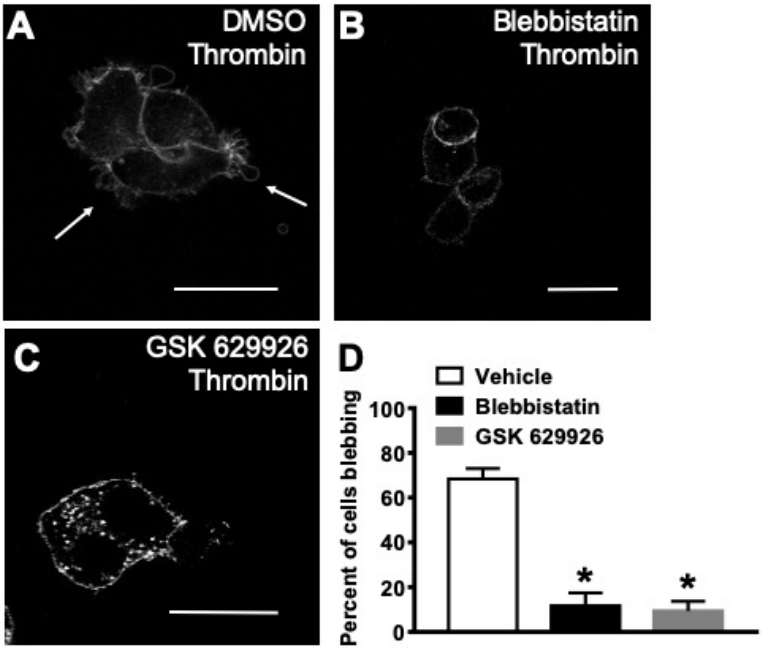

878

879 **Figure 7**

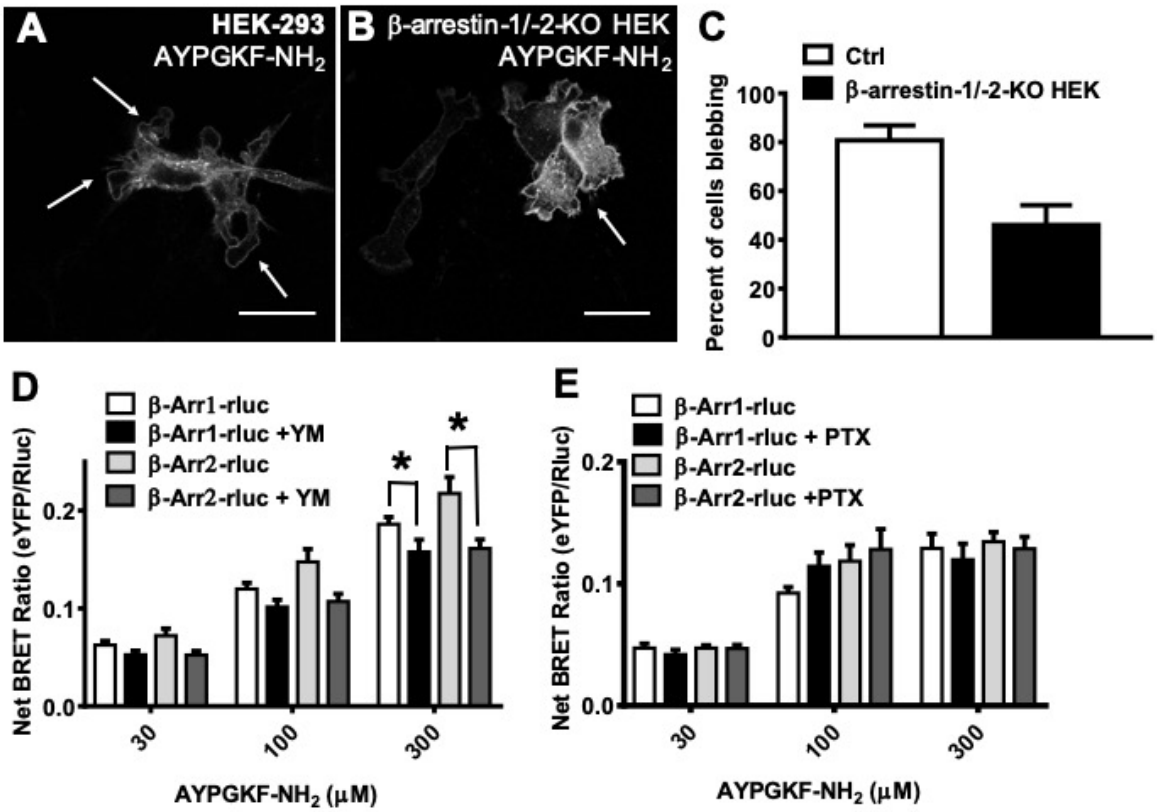

880

881 **Figure 8**

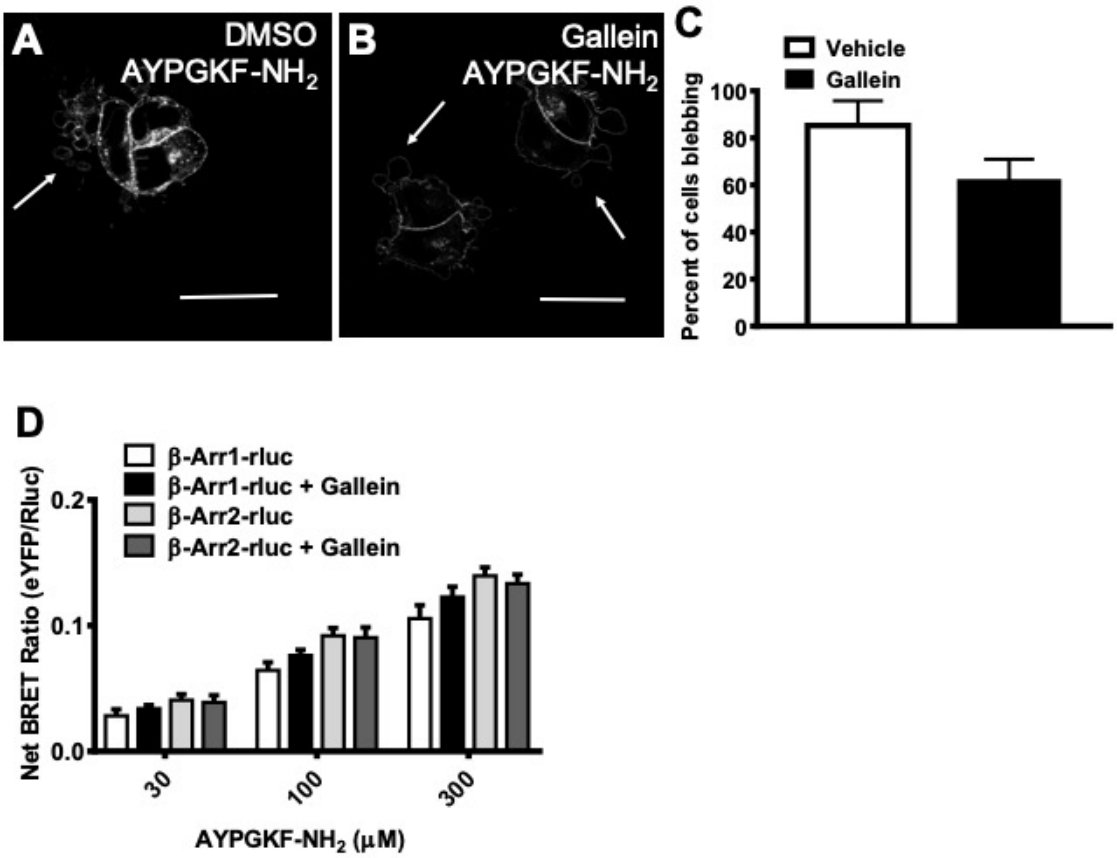

882
883 **Figure 9**

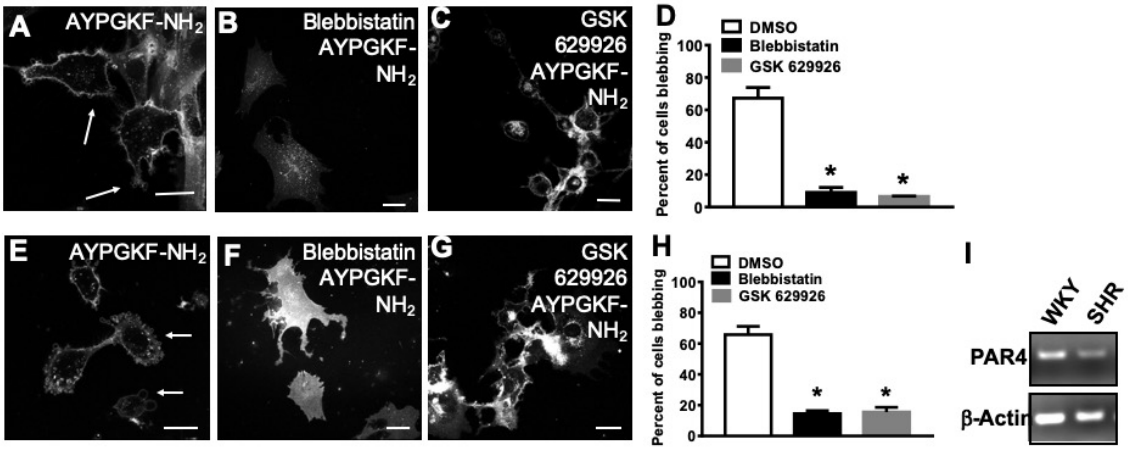
A
AYPGKF-NH2
B
Blebbistatin
AYPGKF-
NH2
C
GSK
629926
AYPGKF-
NH2
D
DMSO
Blebbistatin
GSK 629926
Percent of cells blebbing
100
80
60
40
20
0
*
*
E
AYPGKF-NH2
F
Blebbistatin
AYPGKF-
NH2
G
GSK
629926
AYPGKF-
NH2
H
DMSO
Blebbistatin
GSK 629926
Percent of cells blebbing
100
80
60
40
20
0
*
*
I
WKY
SHR
PAR4
β-Actin

Figure 10

A

Gene Ontology Term	Fold Enrichment
Neuron-neuron synaptic transmission (GO:0007270)	7.69
Natural killer cell activation (GO:0030101)	5.45
Fertilization (GO:0009566)	4.68
Sensory perception of taste (GO:0050909)	4.11
Blood coagulation (GO:0007596)	3.1
Cell-cell adhesion (GO:0016337)	2.81
Sensory perception of chemical stimulus (GO:000760	2.8
Macrophage activation (GO:0042116)	2.78
Blood circulation (GO:0008015)	2.73
Sensory perception (GO:0007600)	2.63

B

Gene Ontology Term	Fold Enrichment
JNK cascade (GO:0007254)	7.88
Anatomical structure morphogenesis (GO:0009653)	3.85
Death (GO:0016265)	3.06
Cell death (GO:0008219)	3.06
Apoptotic process (GO:0006915)	3.01
Intracellular signal transduction (GO:0035556)	2.89
Immune system process (GO:0002376)	2.77
Cell cycle (GO:0007049)	2.36
Developmental process (GO:0032502)	2.22
Signal transduction (GO:0007165)	1.72

Table 1

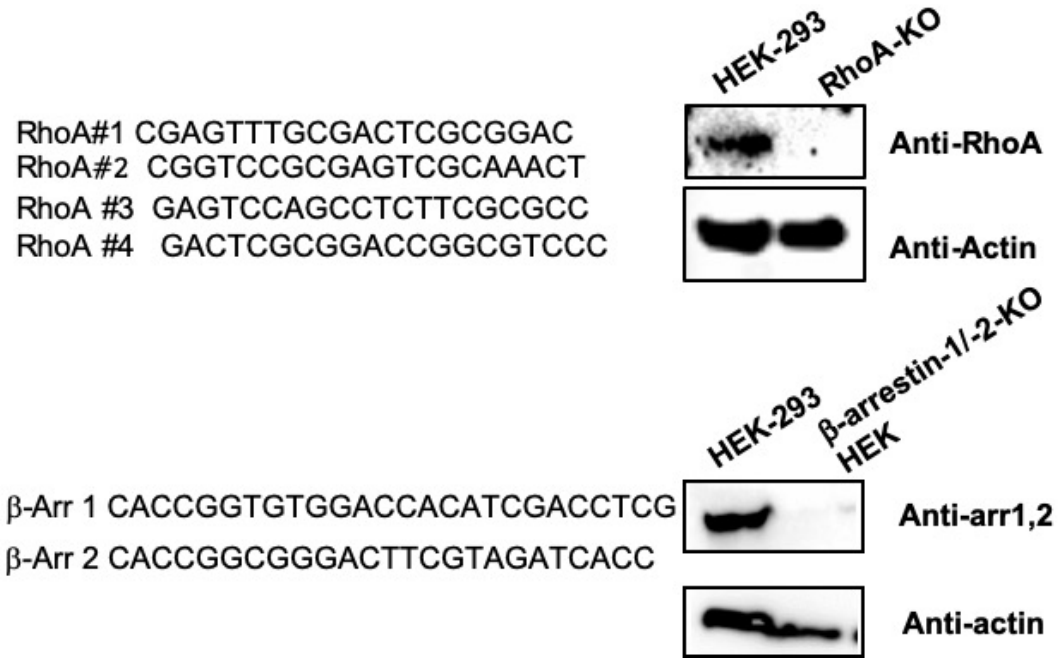

Supplemental Figure 1

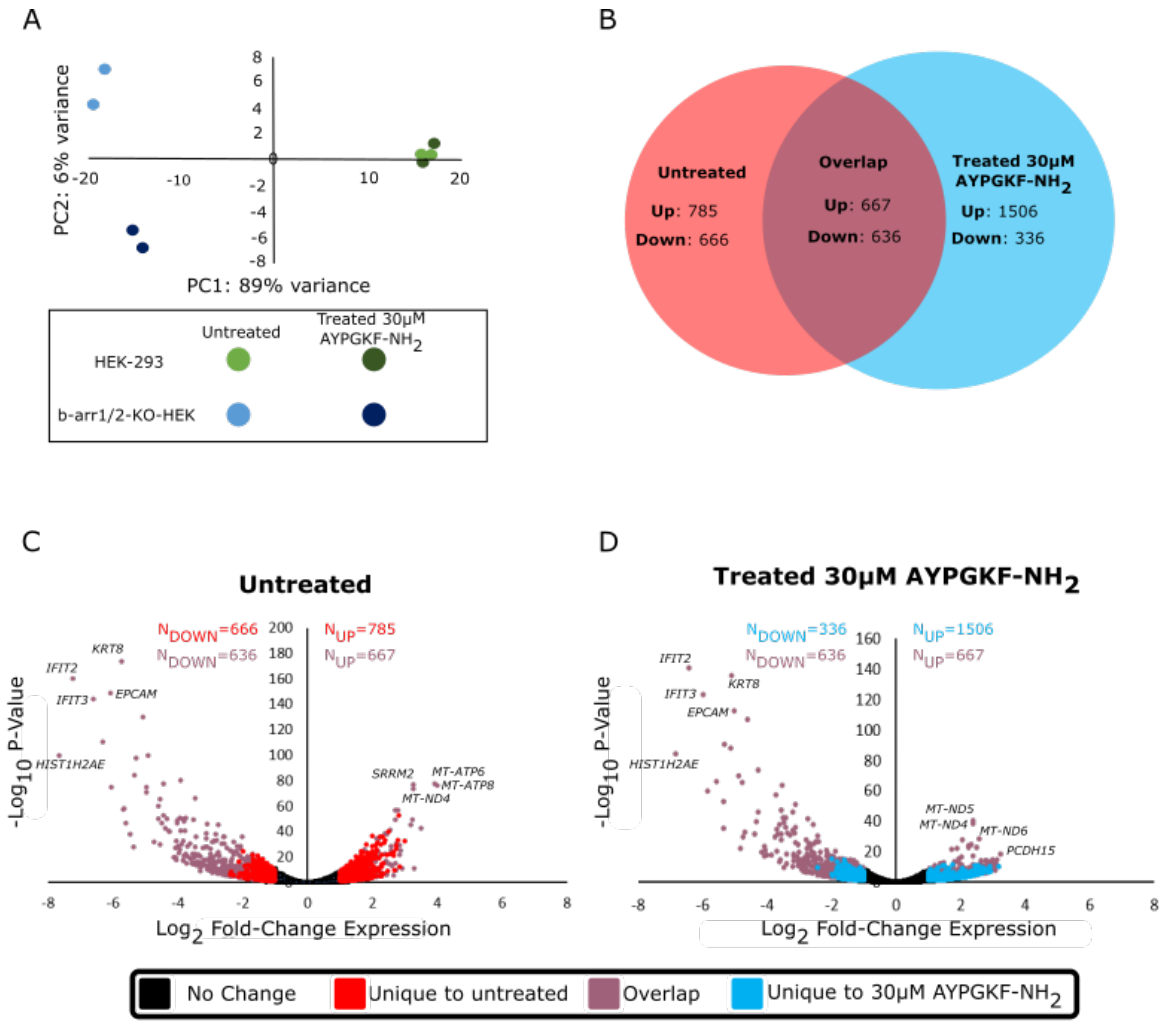

Supplemental Figure 2